Effects of the Growth Rate on the High-temperature Tensile Properties and Micro-organization of Directionally Solidified Ti-44Al-9Nb-1Cr-0.2W-0.2Y Alloys

Yao HUANG [1], **Zhuhang JIANG** [2], **Renheng HAN** [1], **Chengzhi ZHAO** [1, 3] *, **Hexin ZHANG** [1, 3]

[1] *College of Materials Science and Chemical Engineering, Harbin Engineering University, No. 145 Nantong Avenue, Harbin, Heilongjiang, 150001, China*
[2] *Aecc Shenyang Liming Aero Engine Co. LTD, No. 6 Dongta Street, Dadong District, Shenyang City, Liaoning, 110000, China*
[3] *Key Laboratory of Superlight Materials and Surface Technology of Ministry of Education, Harbin Engineering University, No. 145 Nantong Avenue, Harbin, Heilongjiang, 150001, China*

In this experiment, Ti-44Al-9Nb-1Cr-0.2W-0.2Y alloy was prepared by the directional solidification method. The effect of different growth rates on tensile properties and microstructure orientation at high temperature was studied. Three kinds of alloys with different growth rates of 10 μm/s, 15 μm/s and 20 μm/s were prepared. The results show that the tensile properties of the alloy at 800 °C decrease with increasing growth rate, and recrystallization occurred at the position of intracrystal fracture in the microstructure. The size of columnar crystals decreases with the increase of the growth rate, increasing the number of grains and decreasing the orientation difference between the growth and axial directions as well as the preferred orientation of lamellar, and the anisotropy of the material, which leads to the obvious decrease of the tensile strength and plasticity. Combined with electron backscattering diffraction test results, the lamellar orientation of the effective parts of the three specimens after high temperature stretching was studied. It was found that the axial preferred orientation of the alloy specimens decreased obviously with the increase of the growth rate, and the orientation became disorderly and the uniformity of lamellar thickness decreased gradually with the increase of the growth rate. In addition, it was found that a new single-phase γ phase is formed in the microstructure after high temperature stretching, and the distribution range increased with the increase of the growth rate, which seriously degraded the axial preferred orientation of the alloy. It can be concluded that the directionally solidified alloy with a growth rate of 10 μm/s has better microstructure orientation and high temperature tensile properties.
Keywords: directional solidification, growth rate, preferred orientation, high temperature tensile, electron back-scattering diffraction.

1. INTRODUCTION

γ-TiAl alloy, as a new light and high-strength high-temperature structural material, has the advantages of low density, high elastic modulus, high temperature creep and oxidation resistances [1 – 5]. With the addition of high Nb content, the melting point and ordering temperature of TiAl alloy increase [6 – 8]. γ-TiAl alloy is expected to replace part of Ni based alloy, which can be used to manufacture blades, exhaust valves and other aero-engine parts whose operating temperature is not higher than 1000 °C. At present, the main factors restricting its application are low plasticity and difficulty in forming. As an alternative material for turbine blades with light weight and high temperature resistance, directionally solidified TiAl alloy has the disadvantages of high temperature and harsh operating environment. The requirement for reliability in production is far higher than the requirement for cost compression. Therefore, alloying with the proper addition of rare earth elements can effectively improve the microstructure and properties of the alloy. In this paper, based on the high Nb TiAl alloy studied by predecessors,

Ti-44Al-9Nb-1Cr based Ti-44Al-9Nb-1Cr-0.2W-0.2Y alloy was synthesized [9, 10].

The growth stage of directionally solidified samples is mainly divided into initial and stable growth stages, which correspond to the initial solidification nucleation zone and columnar crystal stable growth zone at the front of the solid-liquid interface, respectively. The growth of columnar crystals in the stable growth zone of directional solidification is affected by growth rate and temperature gradient. Since the temperature gradient is quantitative, the main variable studied is the growth rate of directional solidification [11]. The experimental parameter of the growth rate, which is controllable and easy to measure, can be used as the research object to intuitively analyze the directional growth of materials at different growth rates. Moreover, it is easier to find the stable growth range of materials by using medium and high growth rates ($V_L > 10$ μm/s) for directional solidification experiments. In this experiment, three kinds of Ti-44Al-9Nb-1Cr-0.2W-0.2Y alloys with 10 μm/s, 15 μm/s and 20 μm/s growth rates were prepared to study the effect of the growth rate on microstructure orientation and high temperature tensile properties and the mechanism of action (for the convenience of description, directional solidification samples of the three alloys were 410, 420 and 430, respectively). Electron back-scatterring diffraction (EBSD)

---
* Corresponding author. Tel.: +13895718408.
E-mail: *zhaochengzhi@hrbeu.edu.com* (C. Zhao)

technique was used to analyze the microstructure of the alloy after high temperature stretching. The relationship between the growth rate, microstructure, lamellar orientation and tensile properties was explored. The fracture mechanism was analyzed and reasonable improvement suggestions were put forward to study the restricting factors of high temperature properties of directionally solidified high Nb TiAl alloy, providing a reference for subsequent research.

2. EXPERIMENTAL PROCEDURE

The specific composition of Ti-44Al-9Nb-1Cr-0.2W-0.2Y alloy studied in this paper is shown in Table 1, W and Y are added with the atomic percentage of 0.2 %. Three kinds of alloys with growth rates of 10 μm/s, 15 μm/s and 20 μm/s were prepared by the directional solidification method.

Table 1. Chemical compositions of Ti-44Al-9Nb-1Cr-0.2W-0.2Y alloy (units/at.%)

Ti	Al	Nb	Cr	W	Y
Bal.	44	9	1	0.2	0.2

High temperature tensile specimen is obtained by electrospark wire-electrode cutting, and its shape and size are shown in Fig. 1. Since the brittleness of the Ti-Al alloy is obvious at room temperature, no line cutting marks should be left on the surface of the sample during pretreatment and stretching. Before high temperature stretching, a layer of anti-oxidation coating should be evenly coated on the surface of the sample, and then kept at 800 °C for 5 min at a tensile speed of 0.5 mm/min.
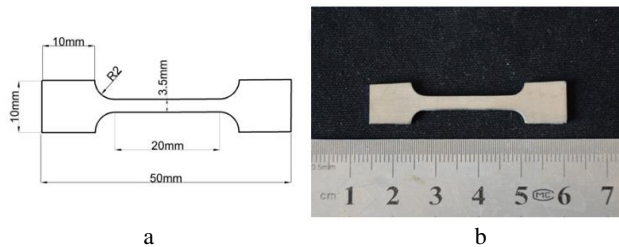
Fig. 1. a – the dimensional drawing of high temperature tensile specimen; b – the picture of high temperature tensile specimen

The three alloy samples were mechanically ground and polished after being stretched at high temperature. Then, the samples were etched using an etchant consisting of a mixture of 15 % HF, 2 % HNO_3, and 83 % H_2O. The etched samples were cleaned and dried immediately, and then observed by SEM. The sections parallel to the tensile direction were selected for the EBSD scanning test for the three kinds of flaky specimens after high temperature stretching. The sample was tested after grinding, polishing and ion etching. The EBSD scan step was set to 1.2 μm.

3. RESULTS AND ANALYSIS

3.1. Effect of growth rate on tensile properties and fracture structure at high temperature

Axial tensile tests at a tensile speed of 0.5 mm/min were carried out on three directionally solidified specimens under different growth rates at 800 °C. The stress-strain curves obtained by equivalent calculation of tensile stress load and histogram analysis of tensile strength are shown in Fig. 2. All the alloys exhibit brittle fracture at high temperature, and only alloys with a growth rate of 10 μm/s exhibit a weak yield phenomenon before tensile fracture. With the increase in the growth rate, the tensile strength and plasticity of the material decrease obviously, but the elastic modulus of different samples is basically the same.

The high temperature tensile curves of directionally solidified specimens with different growth rates show obvious trend and regularity. The growth rate of the grain increases passively with the increase of the growth rate, but the fracture strength decreases obviously. The increase in the directional solidification growth rate reduces the preferred orientation of the material and the axial anisotropy of the mechanical properties of the tensile specimen, leading to degradation of the tensile properties of the alloy at high temperature [12 – 14]. In addition, high β segregation caused by the high growth rate is also an important factor [15 – 17].
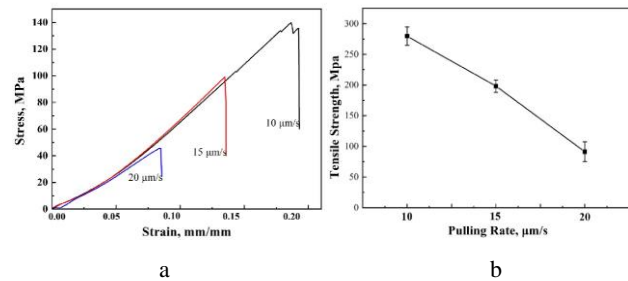
Fig. 2. a – the tensile stress and strain curves at 800 °C; b – the tensile strength line chart at 800 °C

To further probe the relationship between lamellar orientation and mechanical properties, the section of the material after high temperature stretching was scanned and observed. As can be seen from Fig. 3 a, the tensile fracture on the surface is mainly the longitudinal fracture of the lamellar with a small angle when the tensile rate is 10 μm/s. In addition to the longitudinal fracture with lamellar structure, there are also obvious interlamellar fractures. The results show that the fracture degree of the same grain is different at high temperature possibly because of thermal stress or interlayer shear force caused by the length difference of layered structures. In the latter case, there are different lamellar strains of different lengths under the same stress, which results in relative displacement, shear stress and eventual interlamellar cracking [18 – 20]. It can be seen from Fig. 3 b that with the increase of the growth rate, the number of large-angle lamella increases, and obvious oblique cleavage faults appear inside the lamella. There are longitudinal fracture lamellar segments and cleavage steps at the boundary of the multigrain zone. Lamellae at the cleavage step are very thin and have small orientation angles, meaning the gradient of the whole cleavage plane is small. As shown in Fig. 3 c, there exist obvious lamellar cleavage planes perpendicular to the tensile direction, and the smooth cleavage planes are in obvious contrast with the direction of lamellae with small angles. The increase of such cleavage planes is the main reason for the decrease of tensile properties of materials.
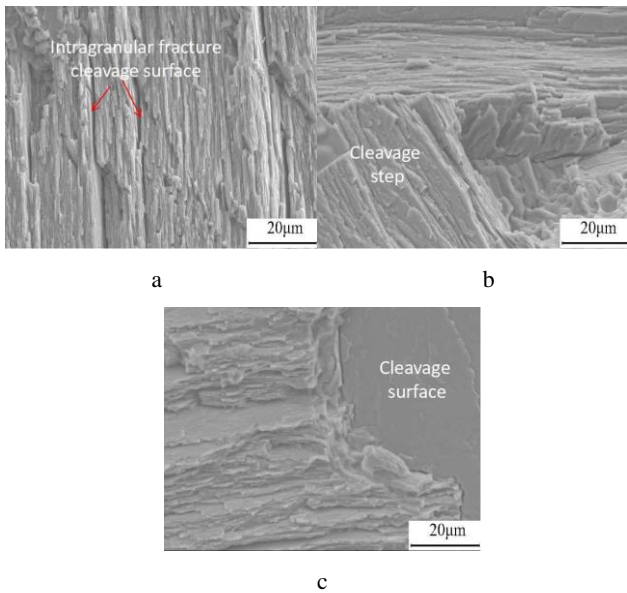
Fig. 3. Fracture morphology of tensile test at different growth
rates: a – 10 μm/s; b – 15 μm/s; c – 20 μm/s

Fig. 4 is a schematic diagram of the fracture of the whole lamellar alloy. Lamellar fracture modes are classified according to different lamellar orientations and tensile directions.
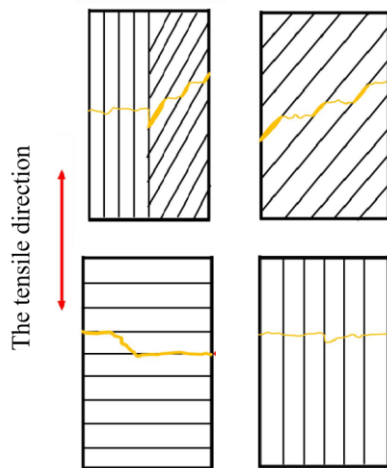
Fig. 4. Schematic diagram of the fracture of fully lamellar TiAl alloy

Tensile strength is highest when the tensile direction is parallel to the lamellar orientation, and the axial tensile force of α_2 and γ lamellar is directly sustained. When the tensile direction is perpendicular to the lamellar orientation, except for dislocation pile-up and grain boundary, only the bonding force between lamellae is resisting tensile. When there is a certain angle between the tensile direction and the lamellar orientation, or there are parallel and vertical positional relations between them at the same time, the interlamellar bonding force is lower than the strength of the lamellar itself, so the cracks are very easy to expand rapidly between the lamellae, resulting in a large range of cleavage fracture. At high temperature, the cleavage fracture trend becomes more obvious with the weakening of the interlamellar bonding force; hence, the lamellar orientation directly affects tensile properties at high temperature [21 – 24].

From the results of the tensile properties of specimens, it can be concluded that the degradation of lamellar orientation is the main reason for the decrease in tensile strength caused by the increase in the growth rate of directional solidification. It is proved that the smaller the angle between lamellar and axial directions, the higher the tensile strength of the material.

3.2. Analysis of microstructure and orientation after high temperature stretching

The heat preservation stage before high temperature stretching is equivalent to heat treatment, and since the high temperature stretching process is carried out at 800 °C, there must be considerable changes in the material microstructure. Axial structures of samples with different growth rates were observed and analyzed after high-temperature stretching at 800 °C, and are shown in Fig. 5.
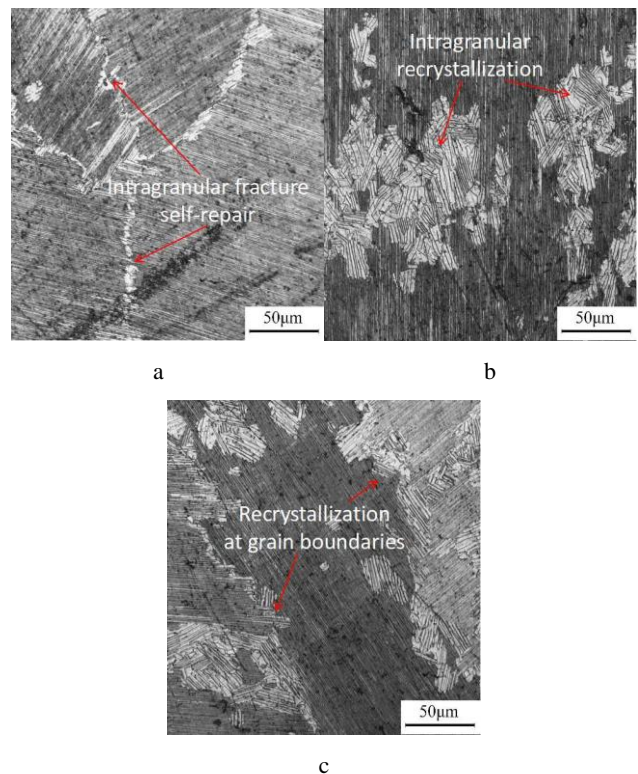
Fig. 5. Morphology of tensile microstructure at 800 °C under
different growth rates: a – 10 μm/s; b – 15 μm/s;
c – 20 μm/s

As shown in Fig. 5 a, lamellar fractures occur at grain boundaries and new phases are formed. The originally separate grains are fractured from the inside due to tensile stress at high temperature. After stress unloading at high temperature, the solid phase transformation of the material leads to the formation of a single-phase γ at the location of the original crack. The original grain changes into more than two grains, and both the newly formed grain boundary and the original grain boundary tend to expand.

Fig. 5 b shows organizational changes that are significantly different from those shown in Fig. 5 a. In the same field of vision, a large number of scattered lamellar structures with broad thickness dominated by single phase γ appear in the original grain, which is different from the one-way precipitation in the nearly lamella. These new

lamellar masses precipitate not at the grain boundary, but within the grain, and have an obvious tendency for nucleation and then growth. The growth of lamellar with the same orientation is not uniform, leading to low growth stability. Under high temperature, there exists an uneven distribution of thermal stress and element composition in the lamellar structure of directional solidification, and the lamella nucleates and grows up induced by stress in the heating and insulation state, but the growth state of the lamella is very unstable, so the lamellar structure with fixed orientation cannot be formed.

It can be seen from Fig. 5 c that, similar to specimen 415, the high temperature tensile microstructure of specimen 420 also has obvious intragranular multi-orientation lamellar clusters and similar grain boundary morphology. However, the multi-orientation lamellar clusters of 420 alloy samples are mainly located at grain boundaries and extend to the surrounding areas. Since the sample was prepared at a higher directional solidification rate, the columnar crystals were fine and β segregation was obvious. As a kind of serious element segregation phase and hard and brittle fracture phase, β segregation exists at the grain boundary and can easily become the core of the formation of a new phase. Hence, the key to this gap must also have something to do with β segregation.

3.3. Orientation analysis of microstructure after high temperature stretching based on EBSD test

The lamellar orientation of the effective part of the specimen after high temperature stretching was studied through the EBSD test. The β phase first generated is the bcc structure, and the lamellar phase is finally obtained on the (100) lattice plane in the same direction as the growth direction should be (111) γ, whose orientation is the preferred orientation of the γ phase. Therefore, judging the preferred orientation of the directional solidification microstructure mainly focuses on two points: 1) Whether the primary phase is β phase solidification; 2) Stability of columnar crystal growth.

Fig. 6 shows the microstructure morphology and inverse pole figure of the alloy specimen after stretching at 800 ℃ obtained by EBSD. The test area is the section near the fracture, and the X direction of EBSD used in the orientation test is the stretching direction. Through analysis of the orientation of the three samples, it can be found that the orientation of the 410 sample is mainly concentrated in the [111] direction. The axial preferred orientation of the 415 sample decreases obviously with the increase in directional solidification growth rate. With the acceleration of the growth rate, the orientation of the 420 sample became disorderly and diversified, and the microstructure showed obvious large-angle lamellar orientation.

Fig. 7 is the pole diagram of the alloy, and the X direction is the axial direction of the alloy tensile test. It can be seen from the results that the 410 specimen has an obvious preferred orientation in the axial direction. With the increase of the growth rate, the preferred orientation of the z-axis direction increases obviously, while the orientation diversification of the 420 sample becomes more serious. EBSD orientation analysis shows that the

directional solidification orientation of the alloy is affected by the growth rate of directional solidification, and the preferred axial orientation decreases with the increase of the growth rate.
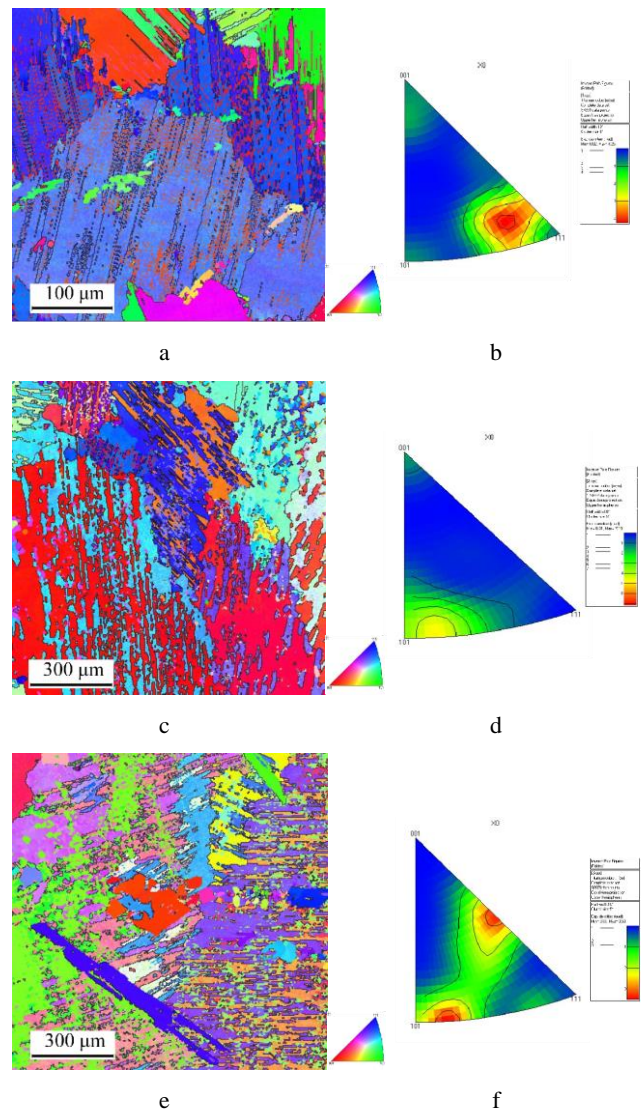
Fig. 6. Orientation diagram and reverse pole diagram of tensile microstructure by EBSD at 800 ℃: a, b – 10 μm/s; c, d – 15 μm/s; e, f – 20 μm/s

Fig. 8 presents the lamellar size analysis of the three alloys. The lamellar thickness of the three alloys after high temperature stretching is concentrated within 20 microns, and the distribution range increases obviously with the increase of the growth rate. This change is in accordance with the microstructure of the alloy lamella. The increase in the growth rate of directional solidification is inversely proportional to the uniformity of lamella thickness.

Fig. 9 shows the grain boundary orientation labeling of the tensile sample at high temperature. The blue parts represent the new single-phase γ generated after high temperature stretching. They aggregate and grow as separate phases in the microstructure, and there is no subgrain boundary under stress in the microstructure. The orientation differences of adjacent grains mainly occur in the range of 0 ~ 2.5 °.
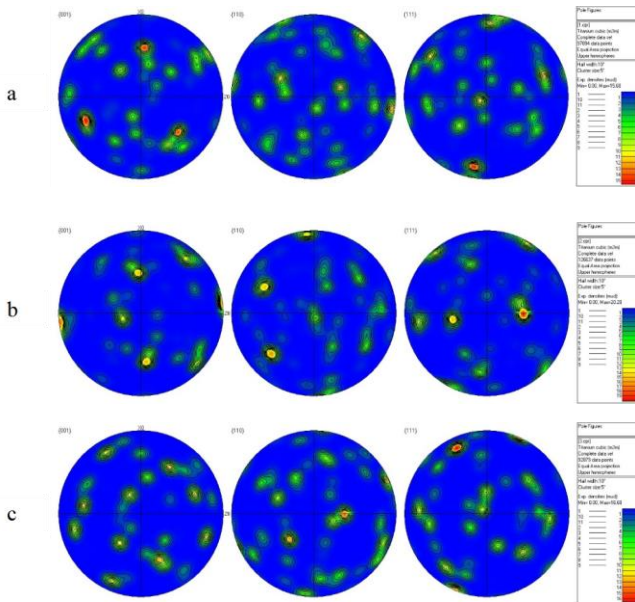
Fig. 7. Orientation pole diagram of the tensile specimens by EBSD at 800 °C: a – 10 μm/s; b – 15 μm/s; c – 20 μm/s
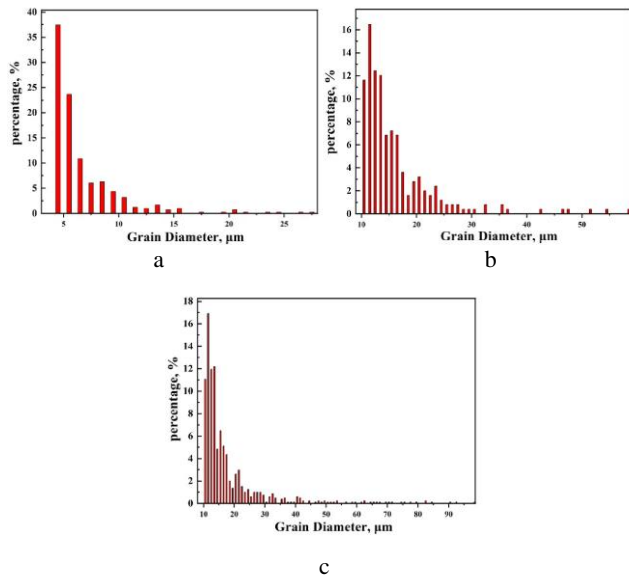
Fig. 8. Lamellar size diagram of tensile specimens at 800 °C: a – 10 μm/s; b – 15 μm/s; c – 20 μm/s

To further study the variation of the precipitated phase at high temperature, the distribution of the precipitated phase in the material was observed, as shown in Fig. 10. With the increase of the growth rate of directional solidification, obvious single-phase γ was precipitated in the microstructure after high temperature stretching, and its distribution and content also changed correspondingly. The precipitated phase formed along the grain boundary with the lower growth rate, and also aggregated and grew up inside the lamellar grain and at the grain boundary with the higher growth rate. Owing to the high growth rate, the solidification rate of the alloy is high, the crystallization process is short, the elements take a lot of time to diffuse, thereby decreasing the thickness uniformity of the alloy lamella, and making the distribution of organizational elements to be non-uniform. Thus, the single phase γ will precipitate and aggregate in the supersaturated lamella in

the crystal. The optimal temperature of lamellar formation in the two-phase zone is 800 °C.
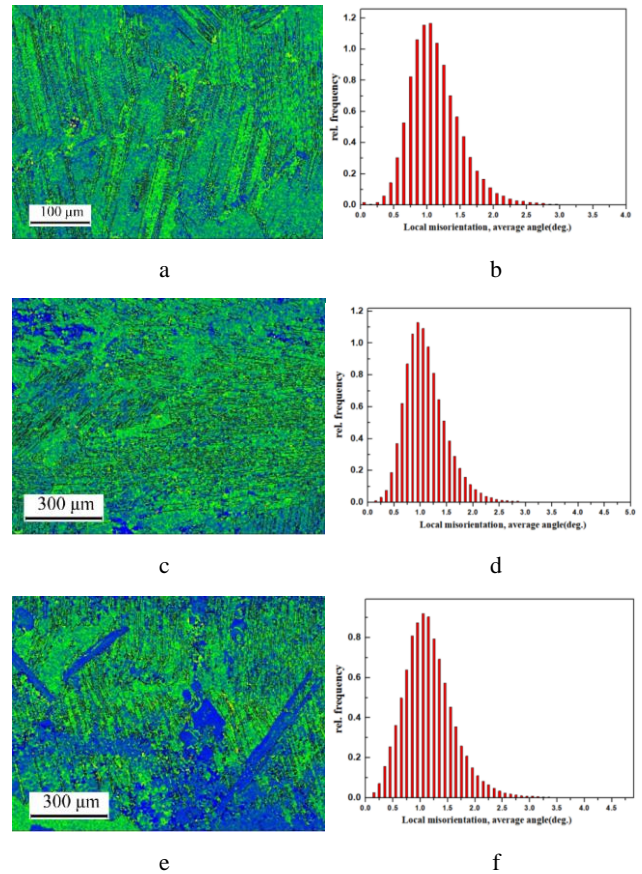
Fig. 9. Grain boundary orientation marking diagram and distribution histogram of tensile specimens at 800 °C: a, b – 10 μm/s; c, d – 15 μm/s; e, f – 20 μm/s

If the alloy served at this temperature has a full lamellar microstructure with incomplete composition diffusion, new phases will be generated and gradually change into a two-state microstructure, which will obviously reduce the strength of the alloy, but correspondingly improve plasticity [25]. However, for directionally solidified materials with high anisotropy, the formation of a single-phase γ without orientation will reduce the preferred orientation of the material, thereby reducing the axial mechanical properties of the alloy.
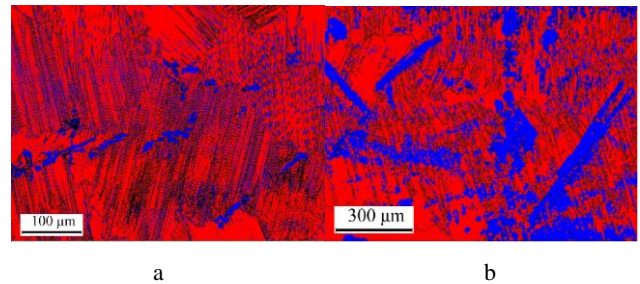
Fig. 10. Distribution of γ phases of tensile specimens at 800 °C: a – 10 μm/s; b – 15 μm/s; c – 20 μm/s

After high temperature tensile, the single-phase microstructure at the grain boundary does not crack directly, but is transformed into small grains with different orientations, which is the recrystallization phenomenon

caused by the joint action of stress and high temperature in the process of high temperature stretching. This phenomenon can be interpreted as a "softening mechanism" of high Nb TiAl alloy at high temperature.

4. CONCLUSIONS

1. In the directional solidification process, increasing the growth rate can refine the size of columnar crystals and grain boundaries, making columnar crystals more inclined to grow in the axial direction, but reducing the preferred orientation of the columnar layer and the uniformity of its size and composition.

2. The angle between lamellar orientation and tensile direction is the main factor affecting the tensile properties of directionally solidified Ti-44Al-9Nb-1Cr-0.2W-0.2y alloy. It can be concluded that the smaller the angle, the better the tensile performance of the material. Higher growth rates reduce the preferred orientation of layered structures, thus lower growth rates are more favourable to realising good mechanical properties.

3. When the growth rate is greater than 10 μm/s, the high temperature mechanical properties of the material tend to decrease with an increase in the growth rate. The high temperature tensile properties are affected by the preferred orientation of columnar crystals in the samples, and the higher the proportion of lamellar crystals with a small axial angle with the specimen, the better the tensile properties. The preferred orientation is affected by the growth rate of directional solidification, and is better at a lower growth rate than at a higher growth rate.

REFERENCES

1. **Han, Y.Q., Lin, C.F., Guo, C.H., Jang, F.C., Chang, X.X.** Fabrication, Interfacial Characterization and Mechanical Properties of Continuous Al_2O_3 Ceramic Fiber Reinforced Ti/Al_3Ti Metal-intermetallic Laminated (CCFR-MIL) composite *Materials Science & Engineering A* 688 2017: pp. 338–345. https://doi.org/10.1016/j.msea.2017.02.024

2. **Lin, C.F., Han, Y.Q., Chang, Y.P., Guo, C.H., Jiang, F.C., Chang, X.X.** Synthesis and Mechanical Properties of Novel Ti-(SiCf/Al_3Ti) Ceramic-fiber-reinforced Metal-intermetallic-laminated (CFR-MIL) composite *Journal of Alloys and Compounds: An Interdisciplinary* 722 2017: pp. 427–437. https://doi.org/10.1016/j.compstruct.2012.12.016

3. **Bolobov, V.I.** Mechanism of Self-Ignition of Titanium Alloys in Oxygen *Combustion, Explosion, and Shock Waves* 38 (6) 2002: pp. 639–645. https://doi.org/10.1023/A:1021132025822

4. **Clemens, H., Mayer, S.** Design, Processing, Microstructure, Properties, and Applications of Advanced Intermetallic TiAl Alloys *Advanced Engineering Materials* 15 (4) 2013: pp. 191–215. https://doi.org/10.1002/adem.201200231

5. **Henaff, G., Gloanec, A.L.** Fatigue Properties of TiAl Alloys *Intermetallics* 13 (5) 2005: pp. 543–558. https://doi.org/10.1016/j.intermet.2004.09.007

6. **Wang, J.Q., Kong, L.Y., Li, T.F., Xiong, T.Y.** High Temperature Oxidation Behavior of Ti(Al,Si)$_3$ Diffusion Coating on γ-TiAl by Cold Spray *Transactions of Nonferrous Metals Society of China* 26 (4) 2016: pp. 1155–1162. https://doi.org/10.1016/S1003-6326(16)64214-0

7. **Chen, G.L., Xu, X.J., Teng, Z.K., Wang, Y.L., Lin, J.P.** Microsegregation in High Nb Containing TiAl Alloy Ingots Beyond Laboratory Scale *Intermetallics* 15 (5) 2006: pp. 625–631. https://doi.org/10.1016/j.intermet.2006.10.003

8. **Chen, Y.Y., Li, B.H., Kong, F.T.** Microstructural Refinement and Mechanical Properties of Y-bearing TiAl Alloys *Journal of Alloys & Compounds* 457 (1) 2007: pp. 265–269. https://doi.org/10.1016/j.jallcom.2007.03.050

9. **Hou, Z.Y., Li, Y.S., Mei, H.J., Hu, K., Chen, G.** Lamellar Morphology of Directional Solidified Ti-45Al-6Nb-xW Alloys *Rare Metals* 35 (1) 2016: pp. 65–69. https://doi.org/10.1007/s12598-015-0631-1

10. **Ryuu, K., Fujita, T.** Effects of W on Mechanical Properties and Microstructure of a Highstrength 9% Cr Heat Resisting Steel *Journal of the Iron and Steel Institite of Japan* 73 (8) 1987: pp. 1034–1040. https://doi.org/10.2355/tetsutohagane1955.73.8_1034

11. **Wang, L., Fan, Q.B., Zhu, X.J., Wang, D.D., Chen, K., Gong, H.C., Qian, Y., Peng, Y., Yang, L.** Effect of Tungsten Micro-Scale Dispersed Particles on the Microstructure and Mechanical Properties of Ti-6Al-4V Alloy *Journal of Alloys and Compounds* 851 2011: pp. 156847. https://doi.org/10.1016/j.jallcom.2020.156847

12. **Kitashima, T., Wang, J., Harada, H.** Phase-field Simulation with the CALPHAD Method for the Microstructure Evolution of Multi-component Ni-base Superalloys *Intermetallics* 16 (2) 2008: pp. 239–245. https://doi.org/10.1016/j.jcrysgro.2011.02.042

13. **Ding, X.F., Lin, J.P., Zhang, L.Q., Su, Y.Q., Chen, G.L.** Microstructural Control of TiAl-Nb Alloys by Directional Solidification *Acta Materialia* 60 (2) 2011: pp. 498–506. https://doi.org/10.1016/j.actamat.2011.10.009

14. **Liu, G.H., Li, X.Z., Su, Y.Q., Chen, R.R., Guo, J.J.** Microstructure and Microsegregation in Directionally Solidified Ti-46Al-8Nb Alloy *Transactions of Nonferrous Metals Society of China* 22 (6) 2012: pp. 1342–1349. https://doi.org/10.1016/S1003-6326(11)61324-1

15. **Liu, D.M., Li, X.Z., Su, Y.Q.** Microstructure Evolution in Directionally Solidified Ti-(50, 52)at%Al Alloys *Intermetallics* 19 (2) 2010: pp. 175–182. https://doi.org/10.1016/j.intermet.2010.08.020

16. **Li, Z.X., Cao, C.C.** Effects of Minor Boron Addition on Phase Transformation and Properties of Ti-47.5Al-2Cr-2Nb alloy *Intermetallics* 13 (3) 2004: pp. 251–256. https://doi.org/10.1016/j.intermet.2004.07.012

17. **Liu, Z.C., Lin, J.P., Li, S.J., Chen, G.L.** Effects of Nb and Al on the Microstructures and Mechanical Properties of High Nb Containing TiAl Base Alloys *Intermetallics* 10 (7) 2002: pp. 653–659. https://doi.org/10.1016/S0966-9795(02)00037-7

18. **Liu, G.H., Li, X.Z., Zhang, Y., Chen, R.R., Su, Y.Q., Guo, J.J., Fu, H.Z., Wang, Z.D., Wang, G.D.** Effect of Growth Rate and Diameter on Microstructure and Hardness of Directionally Solidified Ti-46Al-8Nb Alloy *Transactions of Nonferrous Metals Society of China* 24 (12) 2014: pp. 4044 – 4052. https://doi.org/10.1016/S1003-6326(14)63567-6

19. **Johnson, D.R., Inui, H., Muto, S., Omiya, Y., Yamanaka, T.** Microstructural Development during Directional Solidification of α-seeded TiAl Alloys *Acta Materialia* 54 (4) 2005: pp. 1077 – 1085. https://doi.org/10.1016/j.actamat.2005.10.040

20. **Takeyama, M., Ohmura, Y., Kikuchi, M., Matsuo, T.** Phase Equilibria and Microstructural Control of Gamma TiAl Based Alloys *Intermetallics* 6 (7 – 8) 1998: pp. 643 – 646. https://doi.org/10.1016/S0966-9795(98)00049-1

21. **Zheng, G.L., Jing, J.P.** Effects of Microalloying and Ceramic Particulates on Mechanical Properties of TiAl-Based Alloys *Journal of Materials Science* 41 (22) 2006: pp. 7524 – 7529. https://doi.org/10.1007/s10853-006-0836-7

22. **Boettinger, W.J., Warren, J.A.** The Phase-field Method: Simulation of Alloy Dendritic Solidification during Recalescence *Metallurgical and Materials Transactions A* 27 (3) 1996: pp. 657 – 669. https://doi.org/10.1007/BF02648953

23. **Kim, Y.W.** Ordered Intermetallic Alloys, Part III: Gamma Titanium Aluminides *JOM* 46 (7) 1994: pp. 30 – 39. https://doi.org/10.1007/BF03220745

24. **Jiang, Z.H., Zhao, C.Z., Li, W.D., Zhang, H.X.** Microstructure and Oxidation Behavior of Cr/Mo Modified TiAl Alloy Containing High Nb *IOP Conference Series: Materials Science and Engineering* 205 (1) 2017: pp. 012003. https://doi.org/10.1088/1757-899X/205/1/012003

25. **Xuan, W.D., Liu, H., Li, C.J.** Effect of a High Magnetic Field on Microstructures of Ni-Based Single Crystal Superalloy During Seed Melt-Back *Metallurgical and Materials Transactions B* 47 (2) 2016: pp. 828 – 833. https://doi.org/10.1007/s11663-015-0580-y